Molecular characterization and expression of the gene for mouse NAD^+:arginine ecto-mono(ADP-ribosyl)transferase, *Art1*

Rickmer BRAREN, Gustavo GLOWACKI, Marion NISSEN, Friedrich HAAG and Friedrich KOCH-NOLTE*

Institute for Immunology, University Hospital, Martinistr. 52, D-20246 Hamburg, Germany

Mono(ADP-ribosyl)transferases regulate the function of target proteins by attaching ADP-ribose to specific amino acid residues in the proteins. We have characterized the gene for mouse arginine-specific **A**DP-**r**ibosyl**t**ransferase, *Art1*. Southern blot analyses indicate that *Art1* is a single-copy gene. Northern blot and reverse transcription–PCR analyses demonstrate prominent expression of *Art1* in cardiac and skeletal muscle, and lower levels in spleen, lung, liver and fetal tissues. While human *ART*1 is not represented in the public expressed sequence tag (EST) database, the database contains 14 mouse Art1 ESTs. The *Art1* gene encompasses four exons spanning 20 kb of genomic DNA. The deduced amino acid sequence of Art1 exhibits the characteristic features of a glycosylphosphatidylinositol-anchored membrane protein. It shows 75–77% sequence identity with its orthologues from the human and rabbit, and 33–34% identity with its paralogues from the mouse, Art2-1 and Art2-2. Separate exons encode the N- and C-terminal signal peptides, and a single long exon encodes the entire predicted native polypeptide chain. We expressed Art1 in 293T cells as a recombinant fusion protein with the Fc portion of human IgG1. This soluble protein exhibits enzyme activities characteristic of arginine-specific ADP-ribosyltransferases. The availability of the *Art1* gene provides the basis for applying transgene and knockout technologies to further probe the function of this gene product.

INTRODUCTION

Mono(ADP-ribosyl)transferases (mADPRTs) constitute an important class of enzymes with known regulatory functions as bacterial toxins and metabolic regulators in prokaryotes [1,2]. These enzymes mediate the post-translational modification of specific target proteins by transferring the ADP-ribose moiety from NAD^+ to specific amino acid residues in their target proteins. This usually inactivates the function of the target protein. For example, diphtheria toxin ADP-ribosylates a diphthamide residue in elongation factor 2, thereby shutting off host cell protein synthesis [3]. Cholera toxin and pertussis toxin interfere with signal transduction by ADP-ribosylating the α-subunit of heterotrimeric G-proteins at specific arginine or cysteine residues [2]. In photosynthetic bacteria, an mADPRT (DRAT) regulates nitrogen fixation by ADP-ribosylating an arginine residue of dinitrogenase reductase [4]. Halovibrin, an mADPRT secreted by certain marine bacteria, regulates the developement of the light organ in luminescent fish [5].

Mounting evidence indicates that ADP-ribosyltransferases also play important regulatory roles in higher animals [6,7]. In the mouse, for example, cell-surface mADPRTs have been implicated in regulating myogenesis, long-term potentiation in hippocampal neurons and the activity of cytotoxic T-cells [8–10]. The first mammalian mADPRT was cloned from rabbit skeletal muscle [11]. We have previously mapped the genes for the species orthologues of this gene in the human and the mouse (designated ART1 and Art1 respectively [12]) to a conserved linkage group on human chromosome 11 and mouse chromosome 7, near the genes for the T-cell mADPRTs Art2-1 and Art2-2 [13]. We now report the cloning and characterization of the mouse *Art1* gene.

In the case of *Art2*, defects in gene structure and/or expression have been found to coincide with susceptibility to autoimmune diseases in certain rat and mouse laboratory strains [14–16]. Given the regulatory role of mADPRTs, it is conceivable that defects in other gene family members may also be of clinical relevance. Because of the established transgene and knockout technologies in the mouse, this species is one of the preferred animal models for analysing the functional significance of specific gene defects.

EXPERIMENTAL

PCR primers and PCR reactions

Consensus primers derived from conserved regions of the cDNAs for mouse *Art2-1* and *Art2-2* (EMBL/GenBank accession numbers X52991 and X87612 respectively) and the rabbit and human *ART1* genes (accession numbers M98764 and S74683 respectively) were as follows: B11, CTTTGATGACCAGTACGAGGGCTG; B31, CTTGATAGGGACCCCAAGGCAGGT. Primers derived from the sequence of the mouse *Art1* gene were as follows: M14, GAGGACACCTTCTTCGGTATC; M16, CATGACAGCGGCCCTGCC; M18, CAGCTTTGCCGCCATGGAGAAGGC; M33, GGCAGGGCCGCTGTCATG; M36, CCAGATACCGAAGAAGGTG; M38, CCATAGACGGTCCCAGAGTTCCCTG; M90, GCCTGGTACTACCACTCATACC (see Figure 2). Primers derived from the sequence of the mouse *Art2* gene were as follows: A2F, GAGGACAGAGACCCAGCTGCC; CRE, GACCGAGGAGAACCACAAGGAACAG. Primers derived from the sequence of the

Abbreviations used: EST, expressed sequence tag; GPI, glycosylphosphatidylinositol; hIgG1Fc, Fc fragment of human IgG1; mADPRT, mono(ADP-ribosyl)transferase; RACE, rapid amplification of cDNA ends; RT-PCR, reverse transcription–PCR; UTR, untranslated region.

[1] To whom correspondence should be addressed (e-mail nolte@uke.uni-hamburg.de).

The nucleotide sequence data reported have been submitted to the EMBL/GenBank/DDBJ Nucleotide Sequence Databases under accession number X95825.

human *ART1* gene were as follows: H12, AGCCAATGGCAGGAGCGTCA; H31, CCTGGTGGCACCGGGGTGGA.

PCR reactions were carried out in 20 μl reaction volumes on purified plasmid or P1 DNA (0.1–10 ng) or skeletal muscle cDNA (Clontech; 100–500 ng) in 1 × PCR buffer (Perkin Elmer) with 2.5 units of Amplitaq-Gold polymerase (Perkin Elmer) for 25 cycles (20 s at 95 °C; 20 s at 55 °C; 60 s at 72 °C). Samples were incubated for 8 min at 94 °C prior to the first PCR cycle. For PCR reactions with primers B11 and B31, a 'touch down' protocol was followed, with consecutive decreases in annealing temperature in the first 10 cycles (2 × 60 °C, 2 × 55 °C, 2 × 50 °C, 2 × 45 °C, 2 × 40 °C), followed by 20 cycles with an annealing temperature of 55 °C.

Southern and Northern blot analyses

Genomic DNAs were prepared as described [16] or purchased from The Jackson Laboratory (Bar Harbor, ME, U.S.A.). Genomic DNAs were restriction-digested and subjected to Southern blot analysis essentially as described [16]. Northern blots were purchased from Clontech. A 392 bp fragment of mouse *Art1* was generated by PCR with primers B11 and B31 and was cloned into the pCRII vector (Invitrogen). A 280 bp fragment of the human *ART*1 gene was generated from human genomic DNA with primers H12 and H31 and cloned into the pCRII vector. For use as probes, the respective inserts were purified and radiolabelled to high specific radioactivity (> 10^8 c.p.m./mg) by the random primer labelling procedure [17]. Hybridization and washing were performed under moderate-stringency conditions [16 h in 7 % (w/v) SDS/0.5 M sodium phosphate/1 mM EDTA at 62 °C and 3 × 15 min in 1 % (w/v) SDS/40 mM sodium phosphate/100 mM NaCl at 62 °C]. Bound probe was detected by autoradiography using X-Omat AR films (Kodak) at −80 °C for 2–7 days. This was followed by high-stringency washings [2 × 15 min in 1 % (w/v) SDS/40 mM sodium phosphate at 70 °C] and further autoradiography.

Isolation and sequencing of genomic and cDNA clones

A 129/SvJ mouse genomic P1 DNA library (Genome Systems, St. Louis, MO, U.S.A.) was screened by PCR with primers M16 and M36. Purified P1 DNAs were subjected to restriction digestion with a panel of restriction enzymes, size fractionation by agarose gel electrophoresis and Southern blot analyses. Suitable fragments were obtained by restriction digestion or PCR amplification and subcloned into pBluescript (Stratagene) and pCRII (Invitrogen) plasmid vectors for further restriction mapping and sequence analyses. Mouse heart 'marathon' cDNA was purchased from Clontech and subjected to 5′ and 3′ RACE (rapid amplification of cDNA ends) reactions according to the manufacturer's protocol with nested primers M36 and M33 for 5′ RACE and M16 and M14 for 3′ RACE. cDNA fragments were also amplified with primer pairs M18/M38 and M16/M90. Amplification products were cloned into the pPCRII vector. All sequences were obtained by dideoxy sequence analysis with appropriate vector- and gene-specific primers using the dye-primer and dye-terminator sequencing kits (Applied Biosystems). Sequences obtained from PCR products were confirmed by sequencing clones obtained from two separate PCR reactions.

Amino acid sequence alignment and structure prediction analyses

Multiple sequence alignments, sequence distance and phylogeny calculations were performed with the DNAstar program on a Macintosh computer. Hydrophobicity profiles were determined with the Mac Molly program (Softgene, Berlin, Germany). Database searches were performed with the BLAST programs using the server at www.ncbi.nlm.nih.gov [18].

Reverse transcription–PCR (RT-PCR) analyses

PCR analyses were carried out using cDNAs from different mouse tissues normalized with respect to the transcript levels of six 'housekeeping' enyzmes (MTC panel; Clontech). PCR reactions were performed in 20 μl reaction volumes with the Advantage polymerase mix (Clontech), 0.2 μg of template cDNA and 100 ng of primers derived from two separate exons. The polymerase mix includes the TaqStart antibody (Clontech) for automatic 'hot start' PCR. Conditions were 94 °C for 20 s, 60 °C for 30 s and 72 °C for 180 s for cycles 1–3; the annealing temperature was reduced to 65 °C in cycles 4–6 and to 60 °C thereafter. Aliquots were removed after the 26th, 31st and 36th cycles and analysed by electrophoresis on 1 % (w/v) agarose gels and ethidium bromide staining.

Expression of recombinant Art1–Fc fusion protein and enzyme assays

The coding region of Art1 up to the glycosylphosphatidylinositol (GPI) signal sequence was amplified by PCR with primers F05 (GAGACAGAAGCTTGCCGAGGTCACCTCCACCATGAAGATTCCTGCTATG) and F35 (GGGCTGAGCTCTCGAGATTGCCGGGTGTAGGTGGTCTTGGGGATCCTTTGATGTATTCACAGTTGTATGTACT). The corresponding region of Art3 (accession number Y08027) was amplified with PCR primers F08 (GATATCAAGCTTCGTGAAAAAATGAAGATGGGACATTTTGAAATG) and F38 (TCCTACCAGACTCGAGATTTCCAGGAGTGGGAGGTCTTGGGTTGTAGAGATACCTAGGGTCAATATA). Amplification products were digested with *Hin*dIII and *Xho*I and cloned into a derivative of the pCDM8 expression vector (Invitrogen) containing the coding region for the Fc fragment of human IgG1 (hIgG1Fc; kindly provided by Sandy Zurawski, DNAX Research Institute, Palo Alto, CA, U.S.A.). 293T cells were transfected with purified plasmid (10 μg/5 × 10^7 cells) and Lipofectamine (Gibco/BRL). Cell supernatants were harvested 4 days after transfection.

Recombinant mouse Art2-2 containing the 8-amino-acid FLAG-tag fused to the N-terminus was produced in *Escherichia coli* as described previously [19]. *Neurospora crassa* NAD-glycohydrolase was purchased from Sigma. Affinity-purified rabbit anti-(human IgG1) antibodies were coupled to Aminolink matrix according to the manufacturer's instructions (Pierce). Sepharose-immobilized FLAG-tag-specific monoclonal antibody M2 was purchased from Kodak/ICI [20]. Soluble or immobilized proteins were incubated in 50 μl of 20 mM Tris, pH 8.0, 1 mM ADP-ribose, 5 mM dithiothreitol and 0.5 μCi of ^{32}P-labelled NAD^+ (Amersham) for 60 min at 37 °C. Where indicated, reactions also contained 2 mM agmatine or 5 μg of arginine-rich histones (Sigma). Proteins were analysed by SDS/PAGE and Western blot analyses; supernatants were analysed by TLC as described previously [21,22]. Blots were immunodetected with a mixture of Rt6-specific rabbit serum K48 (1:2000) [23] and rabbit anti-(human IgG) (1:5000) (Pierce). Bound antibody was detected with the enhanced chemiluminescence system (Amersham) using peroxidase-conjugated goat anti-(rabbit Ig) (1:5000). For autoradiography, blots were covered with a black

sheet of paper to quench chemiluminescence and exposed to Kodak X-Omat films for 24 h at −80 °C. Chromatograms were exposed for 4 h at −80 °C.

RESULTS

Cloning of the mouse *Art1* gene

Consensus primers were designed from conserved regions of rabbit skeletal muscle ART1 and murine Rt6 (Art2-1 and Art2-2) [11,23–25]. PCR amplification products obtained with these primers from 129/SvJ mouse genomic DNA were cloned and sequenced. A PCR product obtained with the primer pair B11 and B31 revealed a sequence that was much more similar to the cDNA for rabbit ART1 than to that for murine Art2 (78 % and 45 % nucleotide sequence identity respectively, and 68 % and 34 % identity respectively at the amino acid level). Primers M16 and M36 were derived from this sequence and used to isolate the corresponding gene from a 129/SvJ mouse genomic P1 library by PCR screening. Furthermore, these and the nested primers M14 and M33 were employed for 5′ and 3′ RACE analyses to obtain upstream and downstream coding sequences from BALB/c mouse skeletal muscle cDNA (see Figure 2 for localization of primers).

Structure of the *Art1* gene and its predicted gene product

Figure 1 shows schematic maps of the *Art1* gene and cDNA. Figure 2 shows the nucleotide and deduced amino acid sequences of the *Art1* coding region and the primers used for PCR and sequence analyses. Comparison of the *Art1* cDNA and genomic sequences reveals four exons, spanning 20 kb of genomic DNA. The entire coding sequence for the predicted GPI-anchored cell-surface protein is contained within a single 808 bp exon (exon 3 in Figure 1). Separate exons encode the 5′ untranslated region (UTR) (exon 1), the presumptive N-terminal leader peptide (exon 2) and the hydrophobic C-terminal signal peptide and 3′ UTR (exon 4). The exon/intron structure of *Art1*, therefore, is very similar to that of the rat *Art2* (*Rt6*) gene (Figure 1, left panel) [26].

The *Art1* cDNA sequence was used to search the database of expressed sequence tags (ESTs) [27] for related ESTs with the BLASTn program [18]. Fourteen mouse ESTs were identified that are evidently derived from *Art1* cDNA. The location and orientation of these ESTs are shown in Figure 1 (right panel), with their respective EMBL/GenBank accession numbers. Jointly, these ESTs contain sequences corresponding to each of the four exons, but not additional sequences. The most 5′ EST (W34749) extends two nucleotides further than our longest 5′ RACE product (Figure 1, right panel). The total length of the cDNA is 1401 bp.

The sequence upstream of exon 1 contains a potential TATA box 25 nucleotides upstream of the predicted transcription start site (Figure 2). Similarity searches using the TRANSFAC database of transcription factor binding sites [28] revealed several potential transcription factor binding sites in the 300 bp upstream of exon 1, including sites for MyoD, MEF-2 (myocyte enhancer factor 2) and c-Myb, factors with established roles in muscle cell development [29,30].

Figure 3 shows a comparison of the deduced amino acid sequence of the *Art1* gene product with those of its proposed orthologues from human and rabbit [11,25]. The predicted Art1 amino acid sequence contains deletions of one, two and four residues relative to those of human and rabbit ART1, and extends an additional five amino acids at the C-terminus (Figure 3). Note that mouse, rabbit and human ART1 share an insertion of seven amino acids, one insertion of two amino acids and two single amino acid insertions relative to both Art2 and chicken mADPRTs (diagonally hatched boxes in Figure 3), as well as several additional deletions/insertions relative to Rt6 alone (horizontally hatched boxes in Figure 3). Moreover, mouse Art1

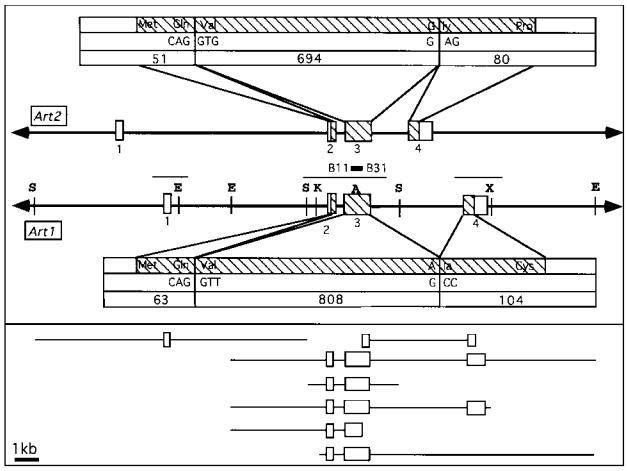

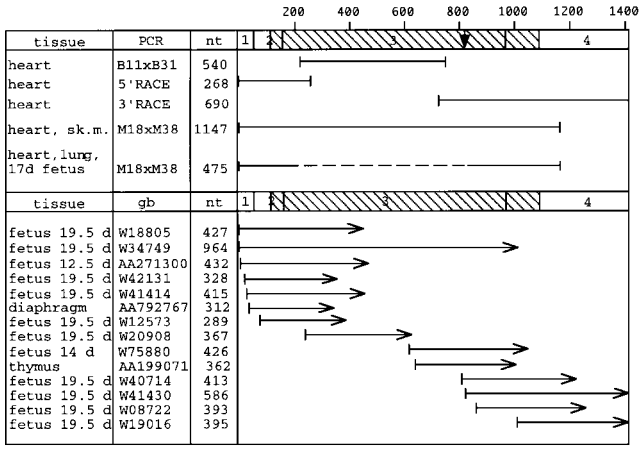

Figure 1 Schematic diagrams of the *Art1* gene and cDNA

Left panel: a map of the *Art1* gene is shown in comparison with the published rat *Rt6* (*Art2*) gene map [26]. Restriction enzyme sites are marked by vertical bars (S, *Sac*I; E, *Eco*RI; K, *Kpn*I; X, *Xho*I; A, *Apa*I). Exons are boxed and coding regions are hatched. The schematic diagrams above (for *Art2*) and below (for *Art1*) the gene maps illustrate the following features of the coding region: N- and C-terminal amino acids, amino acids and codons at splice sites and coding region lengths (in number of bp). The bold line above the *Art1* map marks the position of the fragment that was originally obtained by PCR from genomic DNA with consensus primers B11 and B31. This fragment was used as a probe for the Southern blot analyses shown in Figure 4. Thin lines mark the positions of the three sequenced fragments shown in Figure 2. Fragments obtained by subcloning P1 DNA into plasmid vectors are shown in the lower part of the panel. Right panel: a schematic diagram of *Art1* cDNA fragments obtained by RT-PCR and RACE analyses (upper part) is shown in comparison with *Art1*-specific ESTs from the EST database (lower part). The four exons are boxed and the coding region is shaded as in the left panel. The vertical arrow in the upper part marks the position of a cryptic splice site in exon 3. Tissues from which cDNAs were derived, primers used for PCR and lengths of PCR products are shown in the upper part. Tissue of origin, GenBank accession numbers, lengths and orientation of Art1-specific ESTs are shown in the lower part.

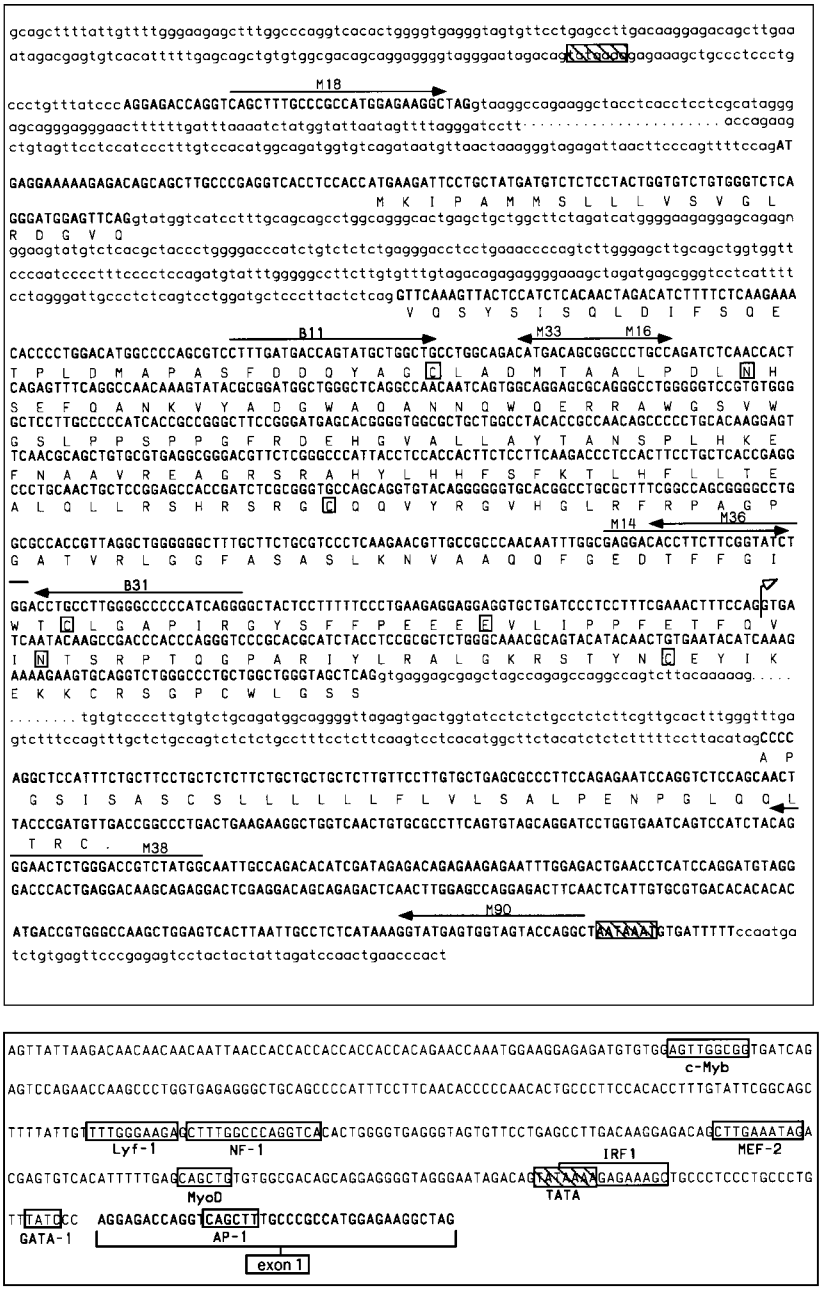

Figure 2 Nucleotide and deduced amino acid sequences of Art1

Upper panel: exon sequences are shown in upper case, and flanking sequences in lower case. Four conserved cysteine residues, the presumptive catalytic glutamic acid residue and two potential N-linked glycosylation sites are boxed. TATA box and polyadenylation signal are shaded (hatching). Positions and orientation of PCR primers are marked by horizontal arrows above the nucleotide sequence. All primer sequences, with the exception of those for B11 and B31, correspond exactly to the shown sequence. The open arrow marks the position of the cryptic splice site in exon 3. Lower panel: potential transcription factor binding sites in and upstream of exon 1, as predicted by a search of the TRANSFAC database [28], are boxed. The predicted TATA box is shaded (hatching). Nucleotides of exon 1 are in bold type.

shows highly significant sequence identity with rabbit and human ART1, even in the N- and C-terminal signal peptides, but no recognizable sequence similarities with the corresponding regions in other mouse, rabbit, human or chicken mADPRTs.

Southern blot analysis indicates that *Art1* is a single-copy gene

Given that two tandemly linked, functional *Art2* genes have been observed in the mouse, but that there is only a single *ART2* gene in the rat [23,31], it was of interest to determine whether the *Art1* gene might also have been duplicated in the mouse and/or rat. To this end we performed Southern blot analyses of restriction-digested genomic mouse and rat DNAs with the B11 × B31 probe from *Art1* exon 3. With genomic DNAs derived from inbred mouse strains, a single band was obtained with each of the enzymes tested, except for *Msp*I, which contains a cognate site within the fragment used as probe (results not shown). In the experiment shown in Figure 4(a), restriction-digested genomic

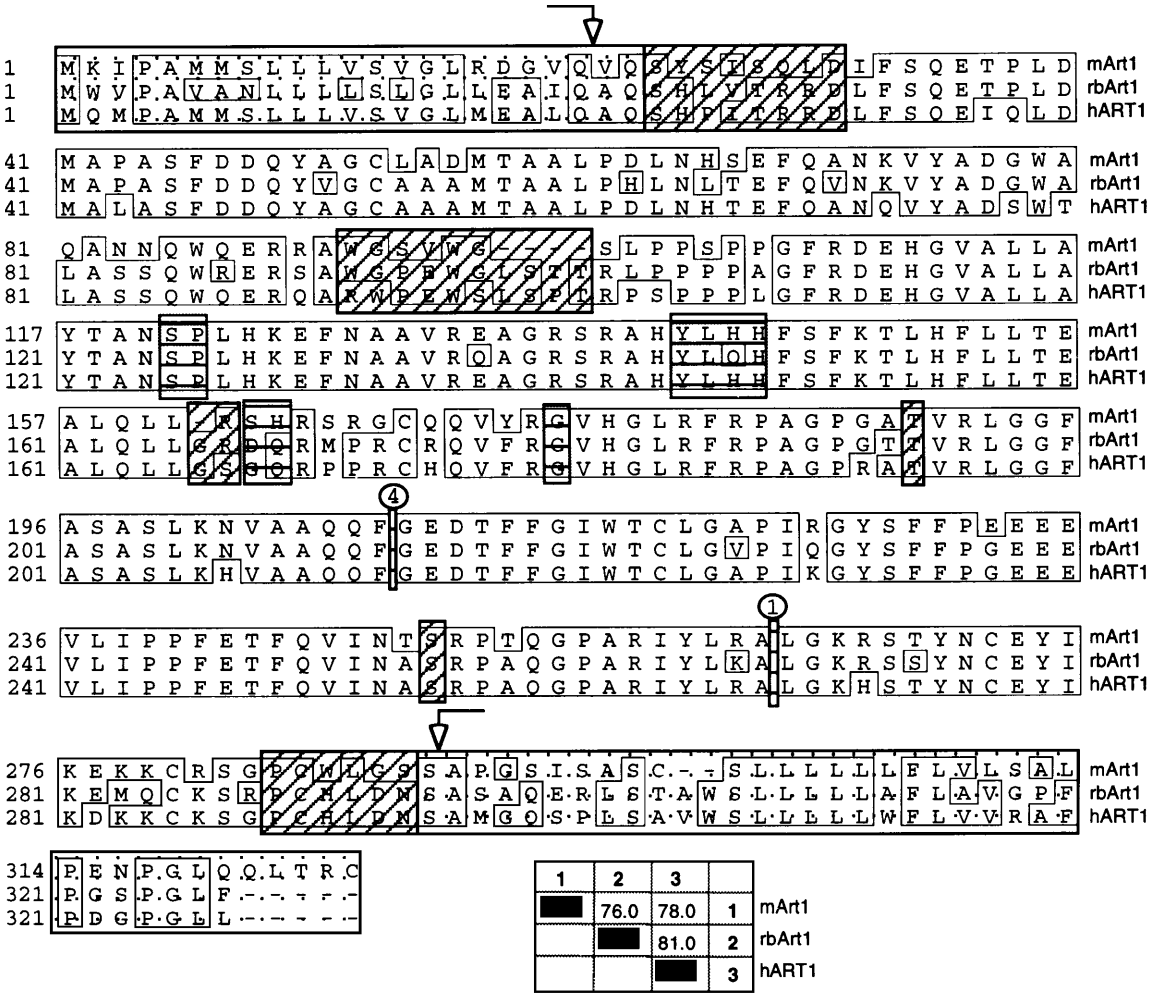

Figure 3 Amino acid sequence alignment of mouse, rabbit and human Art1 proteins

The deduced amino acid sequence of mouse Art1 (mArt1) was aligned with those of its proposed orthologues from rabbit (rbArt1) and human (hART1), and of its paralogues from rodents and chicken (only the alignment with human and rabbit ART1 is shown). Conserved residues are boxed. The hydrophobic N- and C-terminal signal sequences are shaded. Amino acid insertions/deletions relative to rodent Art2 and chicken mADPRTs are marked by diagonal hatching, and amino acid insertions/deletions relative to Art2 alone are marked by horizontal hatching. Circled numbers indicate the number of amino acid residues deleted. Calculated percentage amino acid sequence identities between the Art1 orthologues from mouse, rabbit and human are shown in the box at the bottom. Sequences were compiled from the present study and from database accession numbers X52991, X87616 and M30311 (mouse Art2-1, Art2-2 and rat ART2.2 respectively); M98764 and S74683 (rabbit and human ART1 respectively); D31864 and D31865 (chicken bone marrow AT1 and AT2 respectively); and X82397 (chicken erythroblast mADPRT).

DNA derived from a wild house mouse caught in a farmhouse in Northern Germany (lanes 1–7) was compared with restriction-digested genomic DNAs from the rat cell line EpD3 [32] (lanes 8–12). The blot was probed under conditions of moderate hybridization stringency. Single bands were observed in case of the rat DNA. Remarkably, the house-mouse DNA showed doublet bands with *Hin*dIII and *Pst*I (Figure 4a, lanes 4 and 5). In the experiment shown in Figure 4(b), *Hin*dIII, *Pst*I and *Bam*HI digests of the house-mouse DNA (lanes 1, 4 and 7) were compared with corresponding digests of DNA from inbred C57Bl6/J mice and *Mus spretus*. In each case, the lower band of the house mouse digest corresponded in size to the band of the C57BL/6J mouse digest (lanes 2, 5 and 8), and the upper band to that of the *Mus spretus* digest (lanes 3, 6 and 9). Most likely, the doublets in the house-mouse DNA reflect the presence of two allelic variants of the *Art1* gene in this individual. Note that faint additional bands, possibly reflecting the existence of more distantly related genes, were observed with some enzymes (e.g. Figure 4a, lanes 4, 6 and 7).

The *Bam*HI polymorphism has been used to map the gene in the C57BL/6J × *Mus spretus* backcross panel of DNAs from The Jackson Laboratory [13]. The results demonstrate that *Art1* is closely linked to the *Rt6* genes, near *Hbb* and *Tyr* on mouse chromosome 7.

Expression of the *Art1* gene is most prominent in cardiac and skeletal muscle

In order to determine the expression profile of the *Art1* gene, we performed Northern blot analyses with the B11 × B31 probe. The results show a 1.4 kb *Art1*-specific band in cardiac and skeletal muscle, but not in any of the other tissues analysed (results not shown). For comparison, we performed a similar analysis with a probe derived from the corresponding region of the human

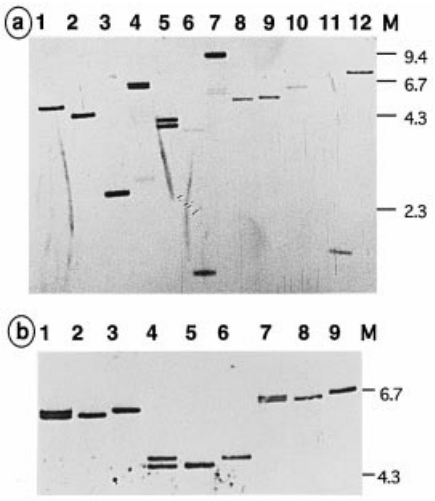

Figure 4 Southern blot analysis of the *Art1* gene

(**a**) Genomic DNAs were digested with *Bcl*I (lane 1), *Stu*I (lane 2), *Sac*I (lanes 3 and 8), *Hin*dIII (lanes 4 and 9), *Pst*I (lanes 5 and 10), *Pvu*II (lanes 6 and 11) and *Eco*RI (lanes 7 and 12), and subjected to Southern blot analysis with the radiolabelled *Art1*-specific probe B11 × B31 (see Figure 1). DNAs were from a farmhouse mouse caught in Northern Germany (lanes 1–7) and from the rat cell line EpD3 [32] (lanes 8–12). (**b**) Genomic DNAs were digested with *Hin*dIII (lanes 1–3), *Pst*I (lanes 4–6) and *Bam*HI (lanes 7–9) and subjected to Southern blot analysis as in (**a**). DNAs were from the same wild mouse as in (**a**) (lanes 1, 4 and 7), C57BL/6J mice (lanes 2, 5 and 8) and inbred *Mus spretus* (lanes 3, 6 and 9). Positions of size markers (kb) are shown on the right.

ART1 gene. The results showed very similar expression patterns of these genes.

Using more sensitive RT-PCR assays, we compared the expression of mouse *Art1* and *Art2* using gene-specific primers derived from separate exons (not shown). The results confirmed that *Art1* expression is most prominent in cardiac and skeletal muscle, while *Art2* is most strongly expressed in spleen. However, low transcript levels could also be detected for both genes in several other tissues, including lung, liver and fetal tissues.

Use of a cryptic splice site in exon 3 yields a truncated Art1 transcript

Unexpectedly, we consistently observed an additional, smaller Art1-specific band when using primers derived from exons 1 and 4 in RT-PCR analyses (results not shown). Cloning and sequencing of this band from three different tissues revealed an alternative splice variant containing a shortened exon 3. This splice variant evidently derives from use of a cryptic splice site in the 3′ half of this exon [this splice site is marked by an arrow in Figure 1 (right panel) and Figure 2 (upper panel)]. This splice variant contains the coding regions for the N- and C-terminal signal sequences and is predicted to encode a truncated, 45-amino-acid long, GPI-anchored polypeptide.

Expression and enzymic analysis of a recombinant Art1–hIgG1Fc fusion protein

We designed a mammalian expression construct for Art1 by replacing the C-terminal GPI signal sequence with a fragment encoding the Fc portion of human IgG1 under the control of the cytomegalovirus promoter. Transfection of this construct into the human kidney cell line 293T led to the appearance of a recombinant protein in the supernatant of transfected cells which

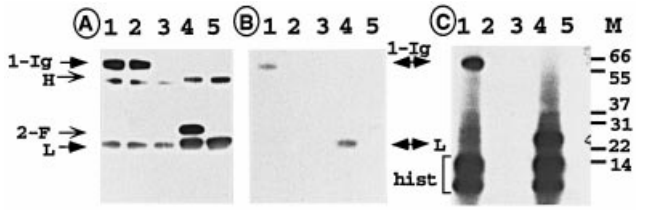

Figure 5 Protein ADP-ribosylation by recombinant mouse Art1 and Art2

Art1–hIgG1Fc (lane 1) and Art3–hIgG1Fc (lane 2) were immunoprecipitated from the supernatants of respective 293T cell transfectants with immobilized rabbit anti-hIgG1Fc antibodies. Art2–FLAG (lane 4) was immunoprecipitated from *E. coli* periplasmic lysates with immobilized mouse anti-FLAG antibodies. Lanes 3 and 5 contain control precipitations using immobilized anti-hIgG1Fc or anti-FLAG antibodies from the supernatants of mock-transfected 293T cells and from periplasmic lysates of mock-transfected *E. coli* respectively. Precipitates were washed, and incubated with [^{32}P]NAD$^+$ for 30 min at 37 °C in the absence (**A** and **B**) or presence (**C**) of 5 μg of arginine-rich histones. Reaction products were size-fractionated by SDS/PAGE and blotted on to a PVDF membrane. (**A**) Immunostain of the blot with a combination of rabbit anti-Rt6 serum K48 (1:2000) and rabbit anti-(human IgG) (1:5000). Bound antibody was visualized by enhanced chemiluminescence using peroxidase-conjugated goat anti-(rabbit IgG) antibodies. (**B**) Autoradiograph of the same blot after quenching of chemiluminescence. (**C**) Autoradiograph of a corresponding gel from an experiment done in the presence of histones. H and L, heavy and light chains of the precipitating antibodies; 1-Ig, recombinant Art1–hIgG1Fc fusion protein; 2-F, recombinant FLAG-tagged Art2; hist, arginine-rich histones. Positions of molecular mass markers (kDa) are shown on the right.

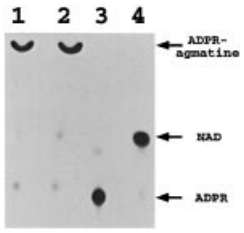

Figure 6 Agmatine ADP-ribosylation by recombinant mouse Art1 and Art2

Art1–hIgG1Fc (lane 1) and Art2–FLAG (lane 2) were immunoprecipitated from 293T cell supernatants and *E. coli* periplasmic lysates respectively, as in Figure 5. Washed precipitates were incubated with [^{32}P]NAD$^+$ for 30 min at 37 °C in the presence of 5 mM agmatine. Protein was precipitated with Strataclean resin and centrifugation, and supernatants were analysed by TLC. Lanes 3 and 4 show control reactions performed in the presence of 1 μg of *N. crassa* NAD-glycohydrolase and with immunoprecipitates from mock-transfected cells respectively. Abbreviation: ADPR, ADP-ribose.

could be precipitated with Protein G–Sepharose and with immobilized goat anti-(human IgG1) antibodies. In Western blot analyses, this recombinant protein reacted with anti-(human IgG1) antibodies (Figure 5A, lane 1).

Figures 5 and 6 show comparative enzyme assays of Art1–hIgG1Fc immobilized on matrix-bound polyclonal goat anti-(human-IgG1) antibodies and FLAG-tagged Art2-2 immobilized on matrix-bound M2 monoclonal mouse anti-FLAG antibodies. The latter serves as a positive control, as we had previously observed that FLAG-tagged Art2 could ADP-ribosylate the light chain of the M2 antibody [22]. Incubation of these immunoprecipitates with [^{32}P]NAD$^+$ led to the covalent incorporation of radiolabel into Art1–hIgG1Fc (Figure 5B, lane 1) and into the light chain of the M2 antibody (Figure 5B, lane 4). Both Art1–hIgG1Fc and Art2-2-FLAG could also ADP-ribosylate arginine-rich histones (Figure 5C, lanes 1 and 4). Control precipitates did not incorporate any radioactivity (Figures 5B and 5C, lanes 2, 3 and 5). When incubated with [^{32}P]NAD$^+$ in the

presence of agmatine (an arginine analogue), both Art1–hIgG1Fc and Art2-2–FLAG catalysed the formation of [^{32}P]ADP-ribosyl-agmatine (Figure 6, lanes 1 and 2). In contrast, *Neurospora crassa* NAD-glycohydrolase catalysed the hydrolysis of [^{32}P]NAD^+ to [^{32}P]ADP-ribose and nicotinamide (Figure 6, lane 3).

DISCUSSION

We have cloned the gene for a mouse mADPRT, *Art1*, and have expressed the Art1 gene product as a soluble enzymically active recombinant fusion protein with the Fc portion of human IgG1. The conclusion that *Art1* is the orthologue of cDNAs previously cloned from skeletal muscle of the rabbit and human [11,25] is based on the following findings. (1) There is conserved chromosomal linkage to the loci for haemoglobin (*Hbb*), Harvey ras (*Hras*) and preproinsulin 2 (*Ins2*) on mouse chromosome 7 and human chromosome 11p [13]. (2) There is a high degree of sequence identity (Figure 3). Note that the sequence similarity extends even into regions encoding the N- and C-terminal signal peptides, where no recognizable similarity with other ADP-ribosyltransferases occurs (Figure 3). (3) Intron/exon boundaries are conserved relative to the human skeletal muscle mADPRT gene (Figure 3; R. Braren, F. Haag and F. Koch-Nolte, unpublished work). (4) The human *ART1* and mouse *Art1* genes show similar patterns of expression.

Two other groups have recently reported cDNAs that evidently derive from the same gene as reported here [33,34]. These cDNAs show 100% sequence identity with exons 2, 3 and 4 in Figures 1 and 2. However, they deviate from our sequence upstream of the border of exons 1 and 2. The sequence of Yu et al. [33] extends for eight residues, and that of Okazaki et al. [34] for 245 residues, upstream of exon 2. These discrepancies could reflect alternative splicing in the 5′ UTR, as has been observed in the case of rat *ART2* gene [26,35]. This raises the interesting hypothesis that differential splicing of the 5′ UTR may be a common mechanism affecting the expression of these enzymes. However, all of our 5′ RACE products from heart and skeletal muscle, as well as the five ESTs extending upstream of exon 2, contained the exon 1 shown in Figures 1 and 2. An oligonucleotide derived from the 5′ sequence of Okazaki et al. [34] did not hybridize to three distinct *Art1*-containing P1 clones. Moreover, BLAST analyses of this sequence revealed that nucleotides 23–192 show 100% sequence identity with the coding region of the cDNA for a ubiquitin-conjugating enzyme (GenBank accession numbers U13175 and AA123113). Thus it is possible that the long 5′ sequence reported by Okazaki et al. [34] represents a cloning artefact, at least in part.

The results of our Southern blot analyses indicate that *Art1*, in contrast with *Art2*, is a single-copy gene in the mouse. The finding that these three genes map near one another on mouse chromosome 7 raises the possibility that they are part of a larger cluster of related genes [13]. Indeed, we have found that at least one additional gene family member (*Art5*) maps to the same chromosomal region (F. Koch-Nolte, G. Glowacki, M. Kühl, F. Haag, M. Cetkovic-Cvrlje and E. H. Leiter, unpublished work). The similarities between *Art1* and *Art2* with respect to their exon/intron structures and sequences probably reflect their derivation from a common ancestor by gene duplication. The existence of species orthologues of *ART1* and *ART2* in the mouse, human and rabbit indicates that the gene duplication event generating the ancestors of *ART1* and *ART2* occurred at the time of or before the mammalian radiation. In contrast, the duplication leading to *Art2-1* and *Art2-2* appears to have been a relatively recent event, probably dating to the time of or shortly after divergence of the rodent lineages leading to the modern rat and mouse [23]. Similarly, two of the three chicken *ART* genes seem to have arisen in a relatively recent gene duplication event [36]. The third known chicken *ART* shows greater sequence divergence, consistent with a more ancient origin [37]. The three chicken *ART* genes do not show any marked similarities in sequence or expression pattern to *Art1* and *Art2*, suggesting that they are paralogues rather than orthologues of these genes.

It is not unreasonable to predict that these genes present the tip of an iceberg, i.e. a larger gene family. Indeed, three additional members of this intriguing gene family have been cloned recently from the human and/or mouse [38–42].

It is of note that the *Art1* and *Art2* genes exhibit restricted expression patterns. Moreover, both genes exhibit relatively low transcript levels, as judged from comparative Northern blot and RT-PCR analyses, i.e. Art1 and Art2 signal intensities are much lower than those for the housekeeping enzymes glyceraldehyde-3-phosphate dehydrogenase and hypoxanthine phosphoribosyltransferase (results not shown). It is conceivable that the low levels and high tissue specificities of *Art* gene expression reflect the need to restrict and control the activities of these presumptive regulatory enzymes. The low representation of Art1 and Art2 in the EST database is consistent with this hypothesis: mouse Art1 is represented by 14 ESTs (Figure 1, right panel), whereas neither human ART1 nor mouse Art2-1 and Art2-2 are yet represented [41].

The availability of the mouse *Art1* gene provides the basis for applying transgene and knockout technologies to further probe the function of its gene product. The mouse will also provide a convenient model for testing whether recombinant Art1 or its inhibitors may be useful tools for experimental interventions. The intriguing hypotheses that this enzyme plays an important regulatory role in endogenous metabolism and that defects in Art1 may be involved in pathogenesis are now becoming accessible to experimental testing.

We thank F. Bazan and G. Dennert for helpful discussions. We also thank G. Dennert for sharing sequence information on *Art1* prior to publication. We thank Maren Kühl, Roman Girisch and Vivienne Welge for excellent technical asssistance. This work was supported by grant no. 310/3-1 from the Deutsche Forschungsgemeinschaft to F.K.-N. The results described here represent in part the graduate thesis of R.B.

REFERENCES

1 Aktories, K. (1991) ADP-Ribosylating Toxins, Springer Verlag, Berlin
2 Moss, J. and Vaughan, M. (1990) ADP-ribosylating Toxins and G Proteins: Insights into Signal Transduction, American Society for Microbiology, Washington, DC
3 Honjo, T., Nishizuka, Y., Hayaishi, O. and Kato, I. (1968) J. Biol. Chem. **243**, 3553–3555
4 Ludden, P. W. (1994) Mol. Cell. Biochem. **138**, 123–129
5 Reich, K. A. and Schoolnik, G. K. (1996) J. Bacteriol. **178**, 209–215
6 Jacobson, M. K. and Jacobson, E. L. (1989) ADP-Ribose Transfer Reactions: Mechanisms and Biological Significance, Springer Verlag, New York
7 Haag, F. and Koch-Nolte, F. (1997) ADP-Ribosylation in Animal Tissues: Structure, Function and Biology of Mono(ADP-Ribosyl)transferases and Related Enzymes, Plenum Press, New York
8 Zolkiewska, A. and Moss, J. (1993) J. Biol. Chem. **268**, 25273–25276
9 Schuman, E. M., Meffert, M. K., Schulman, H. and Madison, D. V. (1994) Proc. Natl. Acad. Sci. U.S.A. **91**, 11958–11962
10 Wang, J., Nemoto, E. and Dennert, G. (1996) J. Immunol. **156**, 2819–2827
11 Zolkiewska, A., Nightingale, M. S. and Moss, J. (1992) Proc. Natl. Acad. Sci. U.S.A. **89**, 11352–11356
12 Haag, F. and Koch-Nolte, F. (1997) Adv. Exp. Med. Biol. **419**, 459–462
13 Koch-Nolte, F., Kühl, M., Haag, F., Cetkovic-Cvrlje, M., Leiter, E. H. and Thiele, H. G. (1996) Genomics **36**, 215–216
14 Greiner, D. L., Mordes, J. P., Handler, E. S., Angelillo, M., Nakamura, N. and Rossini, A. A. (1987) J. Exp. Med. **166**, 461–475

15 Koch-Nolte, F., Haag, F., Kastelein, R. and Bazan, F. (1996) Immunol. Today **17**, 402–405
16 Koch-Nolte, F., Klein, J., Hollmann, C., Kühl, M., Haag, F., Gaskins, H. R., Leiter, E. H. and Thiele, H. G. (1995) Int. Immunol. **7**, 883–890
17 Feinberg, A. P. and Vogelstein, B. (1983) Anal. Biochem. **132**, 6–13
18 Altschul, S. F., Gish, W., Miller, W., Myers, E. W. and Lipman, D. J. (1990) J. Mol. Biol. **215**, 403–410
19 Karsten, S., Schröder, J., da Silva, C., Kahlke, D., Thiele, H. G., Koch-Nolte, F. and Haag, F. (1997) Adv. Exp. Med. Biol. **419**, 175–180
20 Hopp, T. P., Prickett, K. S., Price, V., Libby, R. T., March, C. J., Cerretti, P., Urdal, D. L. and Conlon, P. J. (1988) Biotechnology **6**, 1205–1210
21 Haag, F., Andresen, V., Karsten, S., Koch-Nolte, F. and Thiele, H. (1995) Eur. J. Immunol. **25**, 2355–2361
22 Koch-Nolte, F., Petersen, D., Balasubramanian, S., Haag, F., Kahlke, D., Willer, T., Kastelein, R., Bazan, F. and Thiele, H. G. (1996) J. Biol. Chem. **271**, 7686–7693
23 Hollmann, C., Haag, F., Schlott, M., Damaske, A., Bertuleit, H., Matthes, M., Kühl, M., Thiele, H. G. and Koch-Nolte, F. (1996) Mol. Immunol. **33**, 807–817
24 Koch, F., Haag, F. and Thiele, H. G. (1990) Nucleic Acids Res. **18**, 3636
25 Okazaki, I. J., Zolkiewska, A., Nightingale, M. S. and Moss, J. (1994) Biochemistry **33**, 12828–12836
26 Haag, F., Kuhlenbäumer, G., Koch-Nolte, F., Wingender, E. and Thiele, H. G. (1996) J. Immunol. **157**, 2022–2030
27 Marra, M. A., Hillier, L. and Waterston, R. H. (1998) Trends Genet. **14**, 4–7
28 Wingender, E., Kel, A. E., Kel, O. V., Karas, H., Heinemeyer, T., Dietze, P., Knuppel, R., Romaschenko, A. G. and Kolchanov, N. A. (1997) Nucleic Acids Res. **25**, 265–268
29 Black, B. L., Molkentin, J. D. and Olson, E. N. (1998) Mol. Cell. Biol. **18**, 69–77
30 Gadson, Jr., P. F., Dalton, M. L., Patterson, E., Svoboda, D. D., Hutchinson, L., Schram, D. and Rosenquist, T. H. (1997) Exp. Cell Res. **230**, 169–180
31 Koch, F., Haag, F., Kashan, A. and Thiele, H. G. (1990) Proc. Natl. Acad. Sci. U.S.A. **87**, 964–967
32 Koch, F., Kashan, A. and Thiele, H. G. (1988) Hybridoma **7**, 341–353
33 Yu, Y., Okamoto, S., Nemoto, E. and Dennert, G. (1997) DNA Cell Biol. **16**, 235–244
34 Okazaki, I. J., Kim, H. J., McElvaney, N. G., Lesma, E. and Moss, J. (1996) Blood **88**, 915–921
35 Haag, F., Nolte, F., Hollmann, C. and Thiele, H. G. (1993) Transplant. Proc. **25**, 2784–2785
36 Tsuchiya, M., Hara, N., Yamada, K., Osago, H. and Shimoyama, M. (1994) J. Biol. Chem. **269**, 27451–27457
37 Davis, T. and Shall, S. (1995) Gene **164**, 371–372
38 Koch-Nolte, F. and Haag, F. (1997) Adv. Exp. Med. Biol. **419**, 1–13
39 Levy, I., Wu, Y. Q., Roeckel, N., Bulle, F., Pawlak, A., Siegrist, S., Mattei, M. G. and Guellaen, G. (1996) FEBS Lett. **382**, 276–280
40 Koch-Nolte, F., Haag, F., Braren, R., Kuhl, M., Hoovers, J., Balasubramanian, S., Bazan, F. and Thiele, H. G. (1997) Genomics **39**, 370–376
41 Braren, R., Firner, K., Balasubramanian, S., Bazan, F., Thiele, H. G., Haag, F. and Koch-Nolte, F. (1997) Adv. Exp. Med. Biol. **419**, 163–168
42 Okazaki, I. J., Kim, H. J. and Moss, J. (1996) J. Biol. Chem. **271**, 22052–22057

Received 22 July 1998/7 September 1998; accepted 7 October 1998